ISSN 1028-334X, Doklady Earth Sciences, 2022, Vol. 507, Suppl. 2, pp. S240–S246. © Pleiades Publishing, Ltd., 2022.
Russian Text © The Author(s), 2023, published in Doklady Rossiiskoi Akademii Nauk. Nauki o Zemle, 2023, Vol. 508, No. 1, pp. 24–31.

GEOLOGY OF ORE DEPOSITS

Geochemical and Isotopic Characteristics of Disseminated Sulfide Mineralization of Orogenic Gold Deposits of the Yana–Kolyma Metallogenic Belt, Northeast Russia

Corresponding Member of the RAS V. Yu. Fridovsky[a,*], L. I. Polufuntikova[b,a], and M. V. Kudrin[a]

Received August 22, 2022; revised September 8, 2022; accepted September 9, 2022

Abstract—The results of study of the chemical and S isotopic composition of disseminated pyrite and arsenopyrite from metasomatites of the orogenic Malo-Taryn, Badran, Khangalas, V'yun, and Shumniy gold deposits of the Yana–Kolyma metallogenic belt are presented. Pyrite and arsenopyrite are characterized by a nonstoichiometric composition. Arsenopyrite is enriched in S (an As/S ratio of 0.77–0.99) and contains Sb, Co, Ni, and Cu, the total amount of which is <0.15 wt %. Pyrite contains the same elements (up to 3.71 wt % in total), as well as rare Pb, is depleted in S, and is enriched in As (up to 3.16 wt %). The Ni/Co ratio of pyrite ($10.0 > Ni/Co > 0.1$) is typical of hydrothermal negatively charged pyrite with high conductivity (p-type). It is suggested that the mode of occurrence of invisible Au^{+} in disseminated pyrite and arsenopyrite is mostly isomorphic structurally bounded. The $\delta^{34}S$ values of sulfides of the studied deposits range from –6.4 to +5.6‰, which is characteristic of juvenile/magmatic S sources.

Keywords: pyrite, arsenopyrite, chemical composition, S isotopic composition, orogenic gold deposits, Yana–Kolyma metallogenic belt

DOI: 10.1134/S1028334X2260102X

INTRODUCTION

A significant (often, most) part of gold is invisible in disseminated pyrite and arsenopyrite of proximal sericite–chlorite–carbonate–quartz metasomatites at large orogenic gold deposits (OGDs) of the Yana–Kolyma metallogenic belt (YKMB) [1–4]. The study of isotopic-geochemical characteristics of sulfides from metasomatites allows better understanding of ore-forming processes and the formation of gold mineralization, which is critically important for the re-estimation of the resource potential of known deposits and preparation of programs of searching for large deposits in the YKMB. Here we present the results of studies of the chemical composition and S isotopy of pyrite and arsenopyrite of the Tithonian–Valanginian OGDs of the YKMB. The Malo-Taryn, Badran, and Khangalas deposits are hosted in the Upper Permian–Triassic sedimentary sequences, and the V'yun and Shumniy deposits are associated with the Late Jurassic dikes (151–145 Ma, zircon, U–Pb SHRIMP-II [5]) of trachibasalts, andesites, trachiandesites, dacites, and granodiorites of complex of small intrusions and their exocontacts zones (Fig. 1).

The position of the deposits is controlled by the Adycha–Taryn (Malo-Taryn deposit), Mugurdakh–Selirikan (Badran deposit), Charky–Indigirka (V'yun and Shumniy deposits), and Chai–Yurei (Khangalas deposit) regional faults (Fig. 1). Several mineral assemblages are recognized in vein and disseminated ore bodies: metasomatic pyrite–arsenopyrite–quartz, vein pyrite–arsenopyrite–quartz, gold–polysulfide–quartz, and sulfosalt–carbonate [6]. Our studies [3, 4] and works [2, 7] beyond the known ore bodies and metasomatites of the YKMB OGDs revealed diagenetic (Py1), metamorphic (Py2), and metasomatic (Py3) pyrite and metasomatic arsenopyrite (Apy1).

MATERIALS AND ANALYTICAL METHODS

Samples for mineralogical–geochemical and isotopic–geochemical studies were collected from outcrops and surface/underground mines in various areas of the Malo-Taryn, Badran, Khangalas, V'yun, and Shumniy deposits. The polished sections (74 in total) and grains in epoxy resin (100 sulfide grains in ten polished sections) were prepared for mineralogical, microtextural, and geochemical studies of disseminated sulfide mineralization. The chemical composi-

[a] *Diamond and Precious Metal Geology Institute, Siberian Branch, Russian Academy of Sciences, Yakutsk, 677000 Russia*

[b] *Ammosov Northeastern Federal University, Yakutsk, 677000 Russia*

* *e-mail: fridovsky@diamond.ysn.ru*

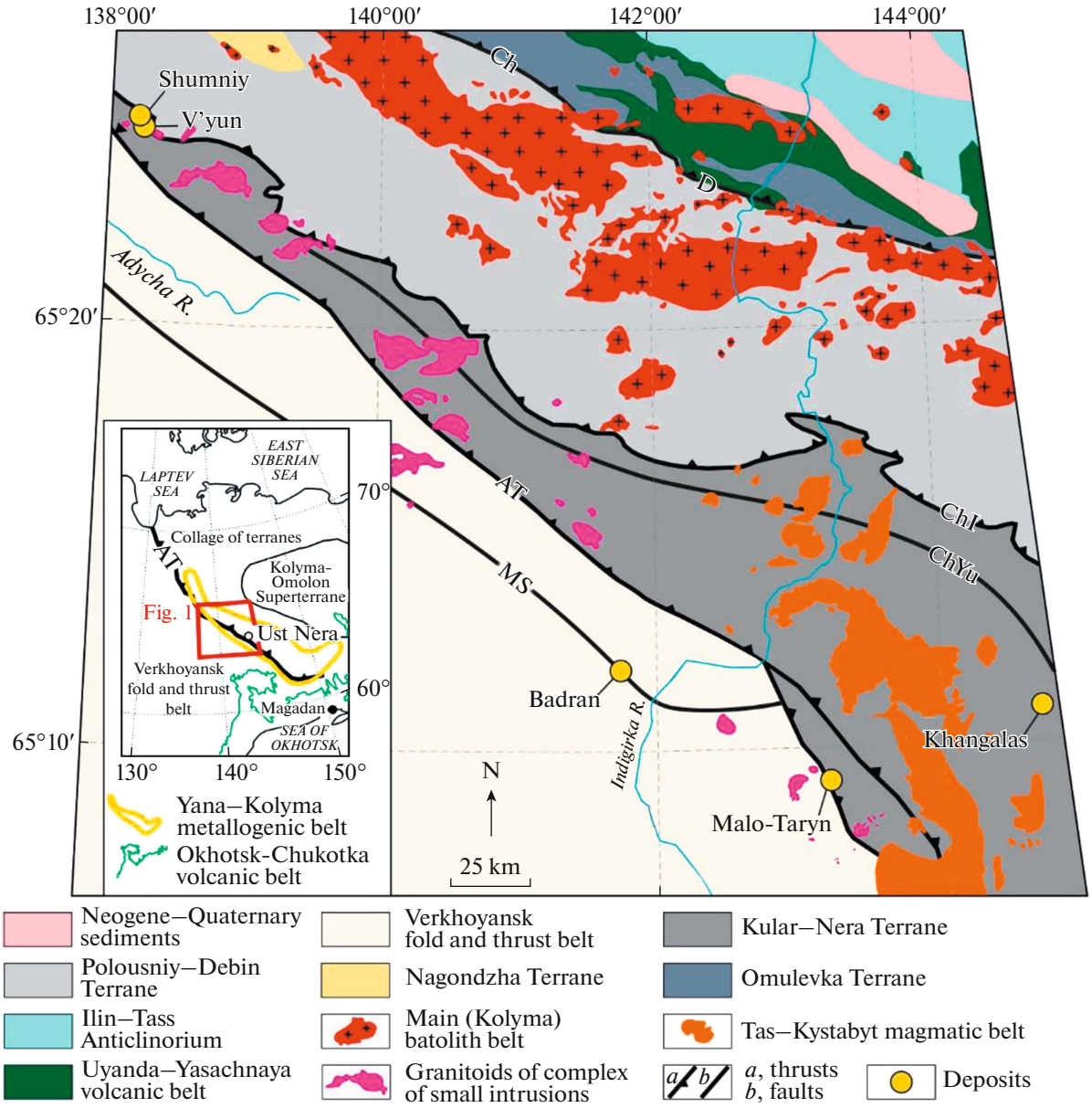

Fig. 1. Scheme of the geological structure of the central part of the Yana–Kolyma metallogenic belt and the position of the studied deposits. Faults: MS, Mugurdakh–Selirikan; AT, Adycha–Taryn; ChYu, Chai–Yurei; ChI, Charky—Indigirka; D, Darpir; Ch, Chibagalakh.

tion of pyrite and arsenopyrite was analyzed at the Department of Physicochemical Analytical Methods of the Diamond and Precious Metal Geology Institute, Siberian Branch, Russian Academy of Sciences (DPMGI SB RAS, Yakutsk, Russia). The chemical composition of pyrite (281 analyses) and arsenopyrite (94 analyses) was measured by profiles using electron microprobe analysis (EMPA) on a Camebax-Micro microprobe (Cameca, Courbevoie, France). The Au contents of >2 ppm were determined in powder monomineral samples using atomic-absorption spectrometry (AAS) with electrothermal dispersion on a MGA-1000 spectrometer (LYUMEKS, Russia). The S isotopic composition ($\delta^{34}S$) of 57 sulfide samples was determined using local and bulk methods in the Laboratory of Stable Isotopes of the Center for Collective Use of the Far East Geological Institute, Far East Branch, Russian Academy of Sciences (FEGI FEB RAS, Vladivostok, Russia) following standard methods published in [3, 4]. The $\delta^{34}S$ values (‰) are given relative to the VCDT international standard. The accuracy of the analysis of S isotopic composition was ±0.20‰ (1σ).

RESULTS AND DISCUSSION

The Au-bearing (up to 159.5 ppm) Py3 and Apy1, the amount of which reaches 4–6%, are the major ore

minerals of proximal sericite–chlorite–carbonate–quartz metasomatites of the studied deposits. Py3 has a cubic and pentagondodecahedral form and zoned structure [3]. Apy1 has a short-prismatic and pseudopyramidal form. The size of the crystals varies from a few to 1.0–1.5 mm (rarely, up to 2–3 mm); the dikes contain metacrystals up to 5 mm in size.

Py3 contains As, Co, Ni, Cu, and rare Sb and Pb; the content of other trace elements is below the EMPA detection limits (Fig. 2a). In Py3 from terrigenous sequences, As is the main trace element (0.31–3.16 wt %) and most analyzed grains (68%) contain 0.5–1.5 wt % As. Pyrite from dikes has the most variable As content: from As-free to 2.03 wt % As (Shumniy deposit) (Fig. 2a). The total content of other trace elements varies from 0.01 to 0.55 wt %, but pyrite grains with a total Co, Ni, Cu, Sb, and Pb content of <0.15 wt % are dominant. The distribution of trace element contents in Py3 from terrigenous rocks and dikes is comparable in some specific features (Fig. 2a). Py3 from the Badran deposit has a higher Sb content (up to 0.21 wt %); the Sb content in Py3 of the Malo-Taryn deposit is below the detection limit (Fig. 2a); Py3 of the Khangalas deposit contains up to 0.11 wt % Pb. Some pyrite crystals from dikes of the V'yun and Shumniy deposits exhibit higher contents of Sb (0.12 wt %), Cu (up to 2.31 wt %), and Ni (up to 3.52 wt %). Py3 from dikes has a negative correlation for $Fe^{2+} \rightarrow Co^{2+}$ and $Fe^{2+} \rightarrow Ni^{2+}$ ($r = -0.7$ to -0.9). Py3 is characterized by zoned As distribution with central (up to 3.07 wt %), intermediate (<2.0 wt %), and marginal (up to 2.20 wt %) zones. The Co and Ni contents can vary significantly within one grain. The higher Co and Ni contents (up to 0.22 and 0.46 wt %) are determined in the central and marginal parts of the crystals, respectively. The empirical formula of Py3 from the studied OGDs is $Fe_{0.98-1.08}(Ni_{0.0-0.01}Co_{0.0-0.01})S_{1.95-2.00}As_{0.01-0.05}$.

Trace elements in sulfides can occur in isomorphic structural-bounded mode and in the form of native nano-/microinclusions [8]. Py3 from the deposits in terrigenous sequences (Malo-Taryn, Badran, Khangalas) and deposits in dikes (V'yun, Shumny) has a nonstoichiometric composition (63% of analyses Fe/S + As ≠ 0.5, S/Fe ≠ 2.00). The S/Fe ratio varies widely in the deposits (V'yun S/Fe = 1.87–2.04; Badran S/Fe = 1.88–2.09). The composition of Py3 differs from the calculated values (46.547 wt % Fe and 53.453 wt % S) indicating the presence of vacant positions in its structure, which are occupied by trace elements. In most analyses, pyrite is depleted in S, the deficit of which is compensated by As^{1-}, but As in a crystal lattice can replace Fe (As^{2+} and As^{3+}) or occurs as nanoinclusions (As^0). Cobalt, Ni, Cu, Sb, and Pb (Me^{2+}) in pyrite isomorphically replace Fe [9]. The As–Fe–S diagram demonstrates the possible scenarios of incorporation of trace elements in the pyrite structure (Fig. 2b). This is the most striking for the S–As couple: higher As contents are typical of the S-deficient pyrite: the S–As correlation for the entire sampling is –0.68 increasing in some objects (–0.77 at the Malo-Taryn deposit and –0.80 at the V'yun deposit). The correlations among Fe, S, and other trace elements vary and are mostly typical of the Malo-Taryn (S–Cu correlation of –0.54) and Shumniy (Fe–Cu correlation of –0.65) deposits.

The variable negative correlations between Co, Ni, and Fe are observed in Py3 of the OGDs in terrigenous sequences (Malo-Taryn, Badran, Khangalas) and dikes (V'yun, Shumniy): from weak ($r = -0.3$ to -0.5) to moderate ($r = -0.65$). The Ni/Co ratio of Py3 widely varies (0.1–19.1), but the Co contents are higher than the Ni contents in most cases, and 90% of analyses exhibit $10.0 > Ni/Co > 0.1$, which is typical of hydrothermal negatively charged pyrite with high conductivity (p-type) [11] (Fig. 2d). The Co-poor Py3 with a Co–Au negative correlation is highly auriferous (Fig. 2e).

The Au content of Py3 varies from 0.3 to 159.5 ppm (Fig. 3a). Observations of microinclusions of native gold are few in number (Khangalas deposit) [4]. The As content is most informative for the assessment of the gold potential of pyrite. The change in the deportment and the content of As in pyrite of gold deposits reflects the evolution of a hydrothermal system. The high Au–As correlation (up to 0.9) is determined for Py3 (Fig. 3b). In the Au–As correlation plot for Py3, the studied deposits are located below the Au saturation line: $C_{Au} = 0.02 \times C_{As} + 4 \times 10^{-5}$ (Fig. 2c) [8]. This indirectly indicates the predominance of the structurally bounded deportment of invisible gold in Py3.

Both Apy1 and Py3 contain Sb, Co, Ni, and Cu, whereas the content of other trace elements is below the EMPA detection limit (Fig. 4a). Their total content varies weakly, but in most grains is no more than 0.15 wt %. The content of some elements is unstable and individual for different objects. Antimony is the main trace element of Apy3 (Fig. 4a). At the Malo-Taryn deposit, Sb comprises 60% of the total amount of trace elements reaching, on average, 85% in Apy3 from dikes and 1.03–1.80 wt % in some samples. The amount of Co is 30–45% of the total amount of trace elements. The Co content of Apy1 from dikes of the V'yun deposit is 0.01–0.06 wt %, whereas the Co content of terrigenous rocks is below the EMPA detection limit. Nickel (0.01–0.30 wt %) and Co (0.01–0.04 wt %) are measured in 65% of the grains analyzed. Apy1 has a nonstoichiometric composition (Fe/S + As ≠ 0.5 in 72% of analyses) and is typically enriched in S (As/S ratio of 0.77–0.99) (Fig. 4b). Apy1 of the Malo-Taryn deposit is most stoichiometric. The main isomorphic substitutions in Apy1 follow the scheme of $S^{1-} \rightarrow As^{1-}$ (r = 0.92–0.99) and $Fe^{2+}(Fe^{3+}) \rightarrow As^{2+}(As^{3+})$ (r = 0.65–0.84). The trace elements in Apy1 (Sb, Co, Ni, Cu) can occur as anion and cation vacant positions in the crystal structure and their distribution in arsenopyrite is more ordered than in

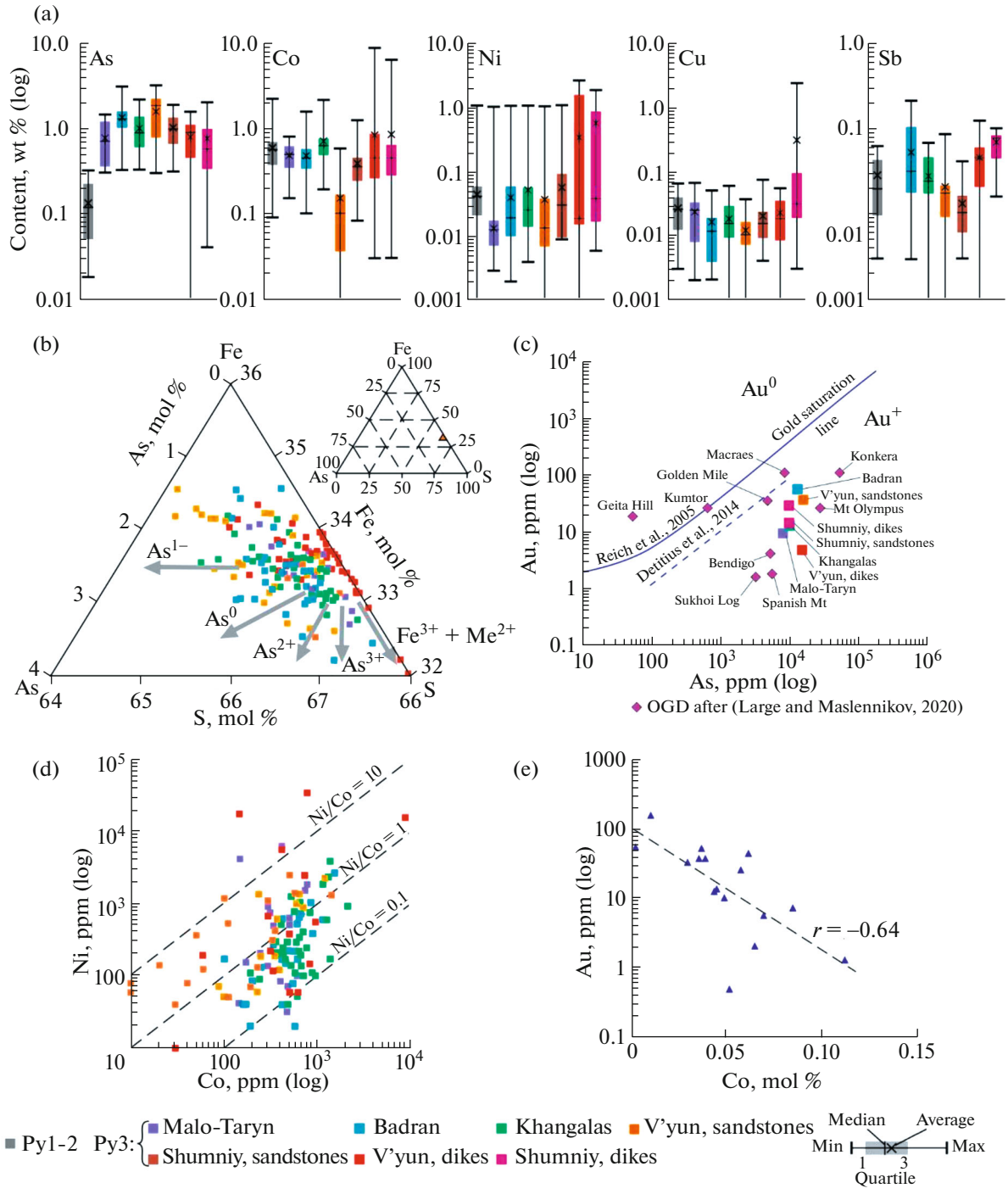

Fig. 2. Variations in the trace element content and ratios of pyrite from orogenic gold deposits of the western part of the YKMB. (a) Distribution of trace elements in Py; (b) As–Fe–S diagram [9] for Py3. Trends of As → S substitution: isomorphic As^{1-} substitution in Py3, nanoinclusions of As^0, As → Fe: isomorphic As^{2+} substitution in Py3, isomorphic As^{3+} substitution in Py3 and two-valent metals (Me^{2+}), which replaces Fe (Co, Ni, Cu); (c–e) correlations in Py3 of the deposits studied: (c) As–Au; (d) Ni–Co; (e) Co–Au.

pyrite. The weak and moderate negative correlations are dominant for the main and trace elements. The As–Sb correlation is the strongest ($r = -0.45$ to -0.61). Arsenopyrite with a nonstoichiometric composition and S excess is typically auriferous [12]. The Au content of Apy1 of the studied deposits reaches 126.3 ppm (Fig. 3a).

One of the possible reasons for the variable S, As, and Fe contents of Apy1 of the studied deposits could be related to the heterogeneous temperature field of

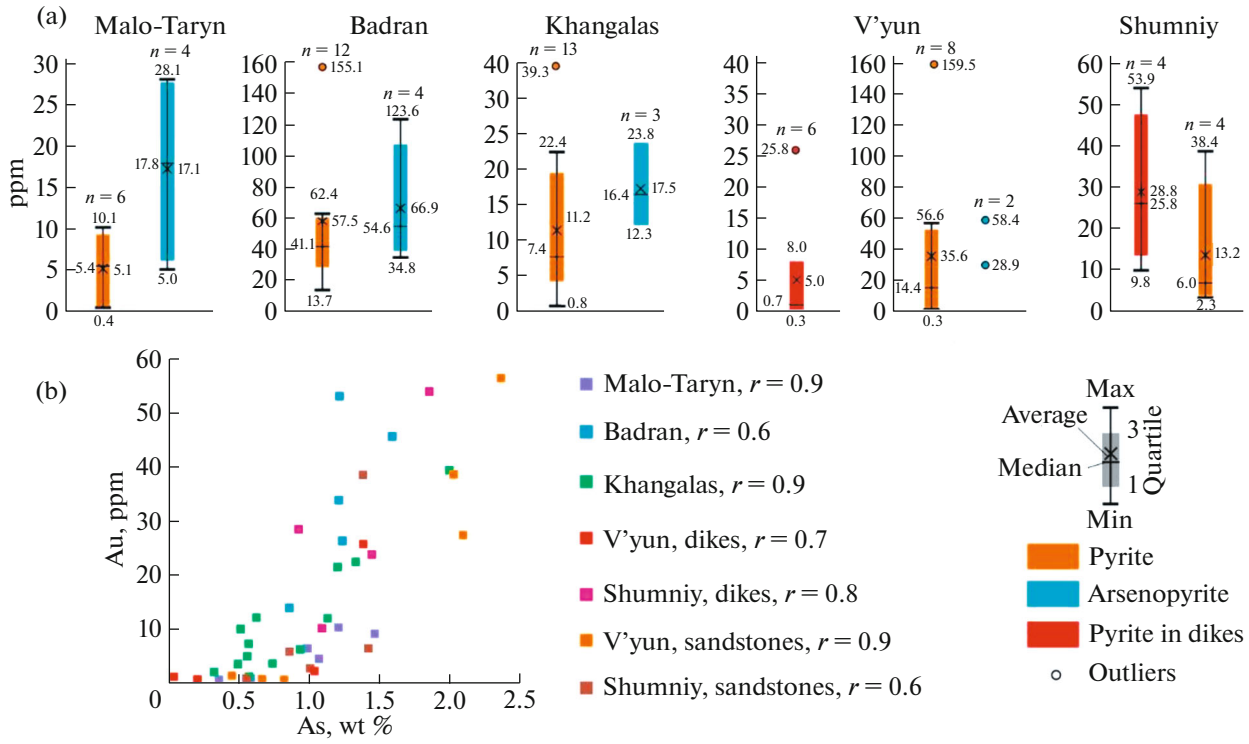

Fig. 3. (a) Au content of sulfides from metasomatites of the studied deposits and (b) As–Au correlation in Py3.

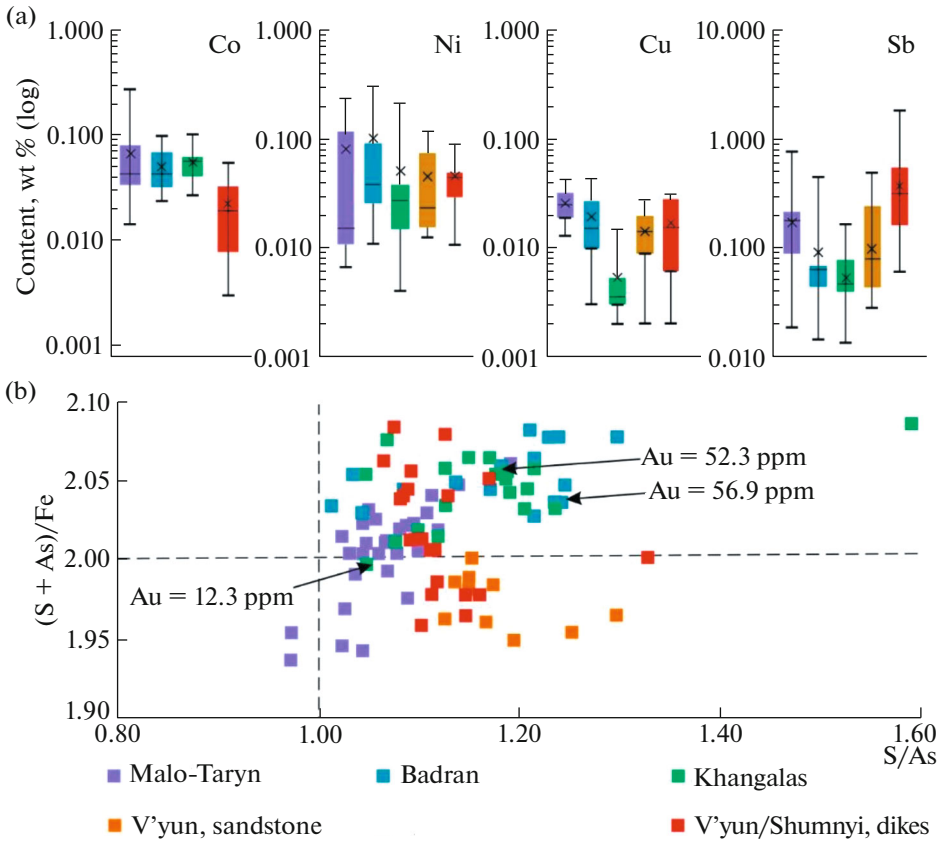

Fig. 4. (a) Distribution of trace elements in Apy1 from metasomatites and (b) S/As–(S + As)/Fe plot of the studied deposits of the YKMB. The interception of lines of S/As = 1 and (S + As)/Fe = 2 corresponds to the stoichiometric composition [13].

Table 1. S isotopic composition of pyrite and arsenopyrite from metasomatites of the studied deposits of the YKMB

Deposit	Mineral	Rock	$d^{34}S_{VCDT}$, ‰	*n*	Source
Malo-Taryn	Arsenopyrite	Sandstones, siltstones	−1.6; −1.4	2	This work
	Pyrite		−5.5; −2.3; 1.4	3	
Badran*	Arsenopyrite	Sandstones, siltstones	−1.1/−0.6; −0.7/−0.8; −0.5/−0.2; −0.4/−0.3; −0.4/0.1; −0.3/−0.3 −0.3/−0.2; 0.0/−0.3;0.3/0.3	18	Fridovsky et al., 2022
	Pyrite		−0.7/1.4; −0.5/1.0; −0.2/−0.3; 0.1/1.8; 0.4/1.6; 0.5/1.8; 0.6/1.9; 0.8/1.1; 1.0/1.2; 1.0/0.7; 1.1/1.0;1.5/1.5	24	
Khangalas	Arsenopyrite	Sandstones, siltstones	−2.1; −1.4; −1.2; −1.1	4	Kudrin et al., 2021 and this work
	Pyrite		−1.9; −1.5; −1.5; −1.3; −0.8; −1.0; −0.6	7	
V'yun	Arsenopyrite	Sandstones, siltstones	4.4	1	This work
	Pyrite		2.3; 3.7; 4.4; 5.6	4	
	Pyrite	Dikes	−6.4; −4.7; − 4.6; −1.9; 3.1; 3.1	6	
Shumniy	Pyrite	Sandstones, siltstones	4.3; 5.0	2	This work
		Dikes	2.1; 2.4; 2.5; 4.8; 5.1	5	

* The values of the S isotopic composition of pyrite and arsenopyrite for the Badran deposit, which are determined by local methods of measurements at the periphery (denominator) and center (numerator) of the grains..

the mineral crystallization, which was also noted for the Blagodatnoe and Olimpiada deposits of the Yenisei Ridge [13]. In the correlation plot with the Au saturation line after [10], the average As and Au contents of Apy1, as well as Py3, are located in the field of isomorphically structural-bounded Au^+ in Apy1.

The studies of the S isotopic composition provide data on the S sources of ore fluids, which is important for understanding the genesis of ore deposits [14–16]. The $\delta^{34}S$ value depends on the involvement of various reservoirs in the formation of ores, variations in physicochemical parameters during the evolution of the ore-forming systems and other factors [16, 17]. The $\delta^{34}S$ values of Py3 of the Malo-Taryn deposit vary from −5.5 to +1.4‰; the $\delta^{34}S$ values of Apy1 are −1.6 and −1.4‰ (Table 1). At the Badran deposit, the $\delta^{34}S$ values of Py3 and Apy1 sampled at different depths (from 587 to 916 m) have a narrow range from −1.1 to +1.9‰. The mostly variable $\delta^{34}S$ values are determined for Py3 (from −0.7 to +1.9‰); the $\delta^{34}S$ values of Apy1 vary from −1.1 to +0.3‰.

The S isotopic composition of sulfides from metasomatites of the Khangalas deposit has a narrow range from −2.1 to −0.6‰: −1.9 to −0.6‰ for Py3 and −2.1 to −1.1‰ for Apy1. A heterogeneous S isotopic composition of sulfides is detected at the V'yun deposit. The highest variations in $\delta^{34}S$ values are determined for Py3 of dikes (from −6.4 to +3.1‰). The $\delta^{34}S$ values of sulfides from terrigenous rocks are +2.3 to +5.6‰ for Py3 and +4.4‰ for Apy. The $\delta^{34}S$ values of Py3 from the Shumniy deposit are positive from +2.1 to +5.1‰. The $\delta^{34}S$ values of Py3 from sandstones and dikes vary from +4.3 to +5.0‰ and from +2.1 to +5.1‰.

The S isotopic composition of sulfides of the studied deposits generally ranges from −6.4 to +5.6‰ (the average $\delta^{34}S$ values for Apy1 and Py3 from terrigenous rocks are −0.4 and +0.8‰, respectively; the average $\delta^{34}S$ values of Py3 from dikes are +0.5‰) (Table 1). These data are in agreement with the results of Gamyanin et al. [6] for sulfides from vein ores of the OGDs of the western part of the YKMB; however, the $\delta^{34}S$ values of sulfides are slightly heavier than from gold–quartz veins of the eastern part of the YKMB (the average $\delta^{34}S$ values for Apy and Py are −3.9 and −4.4‰, respectively) [17]. The similar S isotopic composition of arsenopyrite and pyrite of quartz veins [4, 6] and disseminated ores can indicate their formation during one homogenous evolving hydrothermal event.

CONCLUSIONS

The nonstoichiometric composition of Apy1 and Py3 from proximal metasomatites of the Malo-Taryn, Badran, Khangalas, V'yun, and Shumniy orogenic gold deposits of the Yana–Kolyma metallogenic belt indicates the presence of vacant positions in the crystal structure, which are filled by trace elements and structurally bounded invisible Au^+. Apy1 is enriched in S (As/S ratio from 0.77 to 0.99) and contains Sb, Co, Ni, and Cu (a total content of no more than 0.15%). Py3 contains the same elements (total content of up to 3.71 wt %), rarely Pb, is depleted in S, and is enriched

in As (up to 3.16 wt %). The Ni/Co ratio of Py3 ($10.0 > Ni/Co > 0.1$) is typical of hydrothermal negatively charged pyrite with high conductivity (p-type). The range of $\delta^{34}S$ values for Apy1 and Py3 of −6.4 to +5.6‰ can indicate the involvement of juvenile/magmatic sources in ore formation, but does not exclude the contribution of S to the mineral-forming fluid from sedimentary rocks of orogenic gold deposits of the western part of the YKMB.

FUNDING

This work was supported by a state contract of the DPMGI SB RAS.

CONFLICT OF INTEREST

The authors declare that they have no conflicts of interest.

REFERENCES

1. A. V. Volkov, A. A. Sidorov, V. I. Goncharov, and V. A. Sidorov, Geol. Ore Deposits **44** (3), 159–175 (2002).
2. N. A. Goryachev, O. T. Sotskaya, A. V. Ignat'ev, T. I. Velivetskaya, E. M. Goryacheva, F. I. Semyshev, N. V. Berdnikov, M. A. Malinovskii, and A. V. Al'shevskii, Vestn. Sev.-Vost. Nauchn. Tsentra Dal'nevost. Otd. Ross. Akad. Nauk, No. 1, 11–29 (2020).
3. V. Yu. Fridovsky, L. I. Polufuntikova, M. V. Kudrin, and N. A. Goryachev, Dokl. Earth Sci. **502** (1), S1–S6 (2022).
4. M. V. Kudrin, V. Y. Fridovsky, L. I. Polufuntikova, and L. Kryuchkova, Minerals **11** (4), 403 (2021).
5. V. Yu. Fridovsky, K. Yu. Yakovleva, A. E. Vernikovskaya, V. A. Vernikovsky, N. Y. Matushkin, P. I. Kadilnikov, and N. V. Rodionov, Minerals **10** (11), 1000 (2020).
6. G. N. Gamyanin, V. Yu. Fridovsky, and O. V. Vikent'eva, Russ. Geol. Geophys. **59** (10), 1271–1287 (2018).
7. O. T. Sotskaya, F. I. Semyshev, M. A. Malinovskii, A. V. Al'shevskii, A. E. Livach, and N. A. Goryachev, Vestn. Sev.-Vost. Nauchn. Tsentra Dal'nevost. Otd. Ross. Akad. Nauk, No. **1**, 14–30 (2022).
8. M. Reich, S. E. Kesler, S. Utsunomiya, C. S. Palenik, S. L. Chryssoulis, and R. C. Ewing, Geochim. Cosmochim. Acta **69**, 2781–2796 (2005).
9. N. Román, M. Reich, M. Leisen, D. Morata, F. Barra, and A. P. Deditius, Geochim. Cosmochim. Acta **246**, 60–85 (2019).
10. A. P. Deditius, M. Reich, S. E. Kesler, S. Utsunomiya, S. L. Chryssoulis, J. Walshe, and R. C. Ewing, Geochim. Cosmochim. Acta **140**, 644–670 (2014).
11. R. R. Large and V. V. Maslennikov, Minerals **10** (4), 339 (2020).
12. A. D. Genkin, Geol. Ore Deposits **40** (6), 490–497 (1998).
13. A. M. Sazonov, S. D. Kirik, S. A. Sil'yanov, O. A. Bayukov, and P. A. Tishin, Mineralogiya, No. 3, 53–70 (2016).
14. N. S. Bortnikov, G. N. Gamyanin, V. V. Alpatov, V. B. Naumov, L. P. Nosik, and O. F. Mironova, Geol. Ore Deposits **40** (2), 121–139 (1998).
15. E. O. Dubinina, T. A. Ikonnikova, and A. V. Chugaev, Dokl. Earth Sci. **435** (2), 1665–1670 (2010).
16. R. Goldfarb and D. Groves, Lithos **233**, 2–26 (2015).
17. E. E. Tyukova and S. V. Voroshin, Russ. J. Pac. Geol. **2** (1), 25–39 (2008).

Translated by I. Melekestseva